Superconducting NbN_xC_y thin films fabricated with a dual ion-beam sputtering method

L.-J. Lin and D. E. Prober
Section of Applied Physics, Yale University, New Haven, Connecticut 06520

(Received 23 April 1986; accepted for publication 24 June 1986)

We have fabricated refractory superconducting NbN_xC_y thin films on unheated Si substrates with a low-energy dual ion-beam sputtering technique. Films fabricated with this technique have predominantly $B1$ crystal structure with maximum $T_c \sim 13.2$ K, resistivity of 80–150 $\mu\Omega$ cm and residual resistance ratio ~ 1.0. The use of low ion-beam energies and the absence of substrate heating make this method well suited for producing NbN_xC_y films for superconducting microelectronic applications.

Thin-film δ-phase NbN is an attractive material for superconducting microelectronic and magnet technologies. NbN has a high superconducting transition temperature (T_c up to 17 K), large values of H_{c2}, simple $B1$ crystal structure, and is refractory. Its large superconducting energy gap may allow use of such films in quantum mixer applications for photon detection at larger energies than are possible with elemental superconductors. Recently, several groups have reported fabrication of high-quality δ-phase NbN thin films with $T_c > 14$ K.[1–5] However, most methods utilize intentional substrate heating[1,2(b)–(d),3–5] (200–1100 °C) to obtain best film quality. Such heating is undesirable from a microfabrication point of view, since it can cause degradation of existing underlayer structure (tunnel barriers, films, resists, etc.). In this letter we report the use of a *low-energy* dual ion-beam sputtering technique[6] for producing superconducting NbN thin films on near-room-temperature (typically < 55 °C) Si substrates.

Ion-beam deposition to form NbN has been attempted previously with a *single* ion-beam source in a N_2 atmosphere or with N_2 ions.[7,8] In our own studies[7] using room-temperature (~ 30 °C) substrates, we obtain highly stressed (flaky or non-smooth) NbN thin films. T_c values can approach 11–12 K, but these are multiple or broad superconducting transitions. Other researchers[8] have succeeded with similar systems in making smooth, high-quality NbN films on *heated* substrates.

With the dual ion-beam system, we have previously produced high-quality, smooth and shiny δ-NbN films on near-room-temperature Si substrates.[7] Sharp, single transitions with T_c values up to 11.6 K were obtained using *high-energy* (1500 eV) ion beams with substrate temperatures < 80 °C. The new result in this work is the production of even higher quality films using a *low-energy* (~ 100 eV) dual ion-beam deposition method. These films have further improved superconducting and normal-state properties. We note that with the *dual* ion-beam technique, in general, we find reproducible film properties, in contrast to our results with the single ion-beam system.

A schematic of the sputtering configuration is shown in Fig. 1. This sputtering configuration is a modification of an existing single ion-beam sputtering system[9] in a Pyrex glass chamber with a background pressure of $(1–5) \times 10^{-7}$ Torr. This system has successfully produced high-quality refractory Nb thin films with $T_c \sim 9.1$ K. The first ion-beam source[10] uses Xe gas only. The Xe ions sputter Nb atoms off a Nb target onto a Si substrate [(100) or (111) orientation] which is not intentionally heated or cooled. Meanwhile, the second ion-beam source[11] discharges N_2 or $N_2 + (CH_4$ or Ar) ions to the growing Nb film. The sputtering parameters for the *first* ion source are feedback controlled at $V_{beam1} = 1500$ V and $I_{beam1} = 34$ mA. These parameters give a Nb film growth rate of 2.0–2.3 Å/s. The parameters of the second ion source are varied to optimize the quality of the films, primarily T_c. Sputtering gas flows are precisely controlled by Datametrics electronic valves. The temperature of the substrate holder is < 60 °C after a typical 1.5 h run. The NbN_xC_y growth rate is 1.2–1.7 Å/s.

The NbN_xC_y films fabricated with this technique fall into two general categories, depending on the beam energy of the *second* ion-beam source. Fabrication with *high-energy* N_2 or $N_2 + (CH_4$ or Ar) ions uses a beam voltage V_{beam2} between 1000 and 1500 V, while fabrication with *low-energy* ions uses a beam voltage V_{beam2} between 20 and 200 V. As shown in Fig. 2, the peak T_c value increases as the ion-beam energy of the second ion source decreases, and is maximum for a beam voltage of around 50–100 V. Further reduction of beam voltage reduces T_c, though the films remain smooth and shiny. Figure 2 also shows that $N_2 - CH_4$ ratio control is crucial for achieving highest T_c. Films produced with a $N_2 + CH_4$ mixture have higher T_c than those produced with

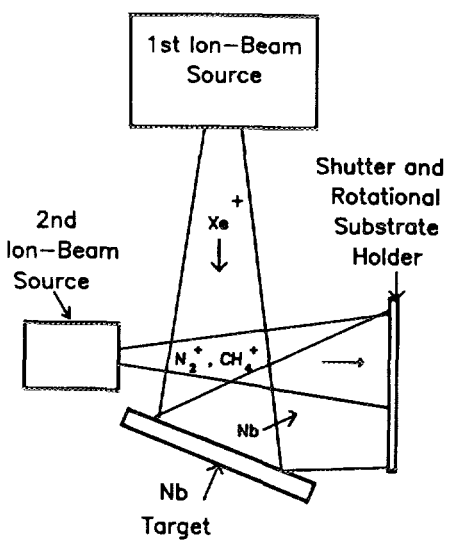

FIG. 1. Schematic diagram of dual ion-beam sputtering system.

 0003-6951/86/330416-03$01.00

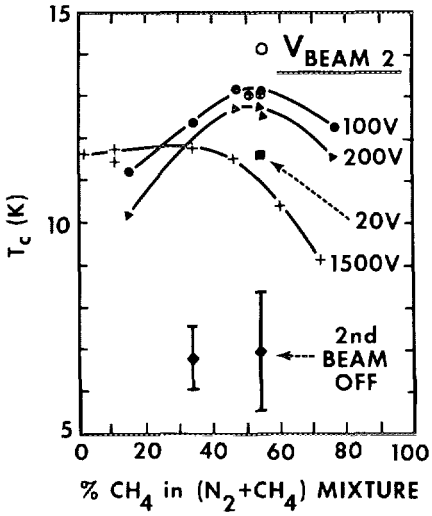

FIG. 2. T_c vs molecular % CH_4 in (N_2 + CH_4) gas mixture. (+) fabrication with 1500 eV N_2 or N_2 + CH_4 ions; (▲) fabrication with 200 eV N_2 + CH_4 ions; (●) fabrication with 100 eV (or 50 eV) N_2 + CH_4 ions; (○) 100 eV ions but with 200 °C substrate temperature; (■) fabrication with 20 eV N_2 + CH_4 ions. Typical ΔT_c for these films is ~0.1 K (see Table I). (◆) fabrication with *single* ion beam in N_2 + CH_4 atmosphere. With a single ion beam and N_2 atmosphere or N_2 in the discharge, T_c values up to 11–12 K are obtained (Ref. 7). Addition of CH_4 reduces film stress. In all single ion-beam cases, multiple or broad transitions are obtained.

N_2 or N_2 + Ar alone. Using a low-energy ion beam, the maximum T_c is ~13.2 K, with a total ion current of the second source optimized at I_{beam2} = 6.4 mA (for ~2.2 Å/s Nb film growth rate). When using a high-energy ion beam, a maximum T_c of ~11.8 K is obtained with optimal I_{beam2} = 3.7 mA. NbN or NbN_xC_y films produced by the dual ion-beam sputtering method show ivory yellow metallic color and are smooth, shiny, and rugged. Heating of the Si substrate to 200 °C during deposition increases T_c by 1 K (see Fig. 2).

The properties of the films were determined with the following methods: van der Pauw four-probe method for T_c and resistivity determination; transmission electron microscopy (TEM) for grain size, crystallographic orientation and lattice constant; Auger depth profile and x-ray photoelectron spectroscopy (XPS) for compositional analysis; electron tunneling with Pb or $Pb_{0.95}Bi_{0.05}$ counter electrodes on native oxide barriers to study the superconducting properties.

Table I lists some typical sputtering conditions and resulting film properties. A common feature of these films is the very small grain size, <70 Å. This result has also been seen by other groups when fabricating NbN on low-temperature (<100 °C) substrates.[2(a),2(b)] The lattice constant a_0 is 4.38 Å for δ-phase NbN and up to 4.46 Å for NbN_xC_y films.[1(a),2(c)-4] Our findings for a_0 for our NbN_xC_y films (calculated from TEM diffraction patterns) range between these two values, with a_0 increasing as the energy of the N_2 ions decreases (at the peak T_c).

The films fabricated with high-energy ions (samples A and B) appear to be δ phase, as indicated by the strong (200) diffraction intensity which has also been seen by other workers.[1(a),2(a),2(c),3,7] Even though samples A and B have different amounts of carbon in each film, the relative N/Nb atomic ratios (0.92 and 0.94) remain close to the value for δ-phase NbN.[12] For samples D and E the TEM diffraction patterns reveal (220) to be the strongest diffraction plane. This may arise from a mixture of the *B* 1 and tetragonal crystal structures, since the distance between (220) diffraction planes is the same (1.551 Å[2(e)]) for these two structures. It is also possible that films fabricated with low-energy ions may have a preferred (220) orientation of *B* 1 crystallites.

Samples D and E show weak metallic behavior (residual resistance ratio $RRR = R_{300\ K}/R_{20\ K} \sim 1.0$). They also have higher T_c and lower resistivity than samples A and B. These factors together give a smaller calculated magnetic penetration depth,[3(a)] λ = 250–285 nm. Small values of λ are preferable for microelectronic applications. (The intrinsic magnetic penetration depth for NbN is ~200 nm.[3(a)]) NbN films fabricated on near-room-temperature Si substrates and possessing the desirable combination of resistivity <80 $\mu\Omega$ cm, RRR ~ 1.0, T_c > 12.5 K and λ < 300 nm have not been obtained in previous studies.

We have also investigated the quasiepitaxial growth[5] of polycrystalline NbN on unheated (100) orientation MgO single-crystal substrates.[13] The close lattice match of (100) MgO substrates to δ-NbN may favor oriented NbN growth in the δ phase.[14] Fabrication using *high-energy* N_2 + (CH_4 or Ar) ions on these substrates causes T_c to increase ~0.5 K over the value for silicon substrates. Using *low-energy* N_2 + Ar ions, T_c increases from ~10 to ~11.4 K, but T_c remains the same for N_2 + CH_4 mixtures. Thus, the substrate effect on film growth is not significant for *low-energy* deposition using N_2 + CH_4 mixtures.

Tunneling studies were conducted on films fabricated with high-energy[7] and with low-energy ions. Figure 3 shows a typical tunneling *I-V* curve for a high T_c film fabricated with low-energy ions. The film in this figure with T_c = 14.1 K was deposited on a Si substrate with T_{sub} = 200 °C. The *I-*

TABLE I. V_{beam2} is the beam energy of the second ion source. I_{beam2} denotes the total ion current from the second ion source. * : N_2/Ar mixture, with flow rates of 2.1/0.57 sccm. The magnetic penetration depth λ is calculated with the equation given in Ref. 5 using a $2\Delta/kT_c$ value of 3.9. The atomic composition ratio is from Auger depth profile analyis. a_0 denotes lattice constant. Diff. denotes the strongest diffraction plane with electron beam diffraction. Typical film thickness is 1000 Å.

Sample	V_{beam2} (V)	I_{beam2} (mA)	P_{N_2} (μTorr)	N_2/CH_4 flow (sccm)	T_c (K)	ΔT_c (K)	$\rho_{20\ K}$ ($\mu\Omega$ cm)	RRR	λ (nm)	Nb/N/C ratio	a_0 (Å)	Diff.
A	1500	3.1	58	2.1/0.34	11.7	0.10	120	0.89	320	1:0.92:0.68	4.38	(200)
B	1000	4.1	58	*	11.2	0.09	158	0.92	375	1:0.94:0.17	...	...
C	200	6.4	42	1.5/2.5	12.4	0.06	156	0.99	356	1:0.64:0.64	...	...
D	100	6.3	42	1.5/2.5	12.7	0.09	77	1.02	246	1:0.60:0.88	4.41	(220)
E	≲100	6.2	42	1.5/2.5	13.0	0.16	105	1.01	284	1:0.60:0.59	4.46	(220)

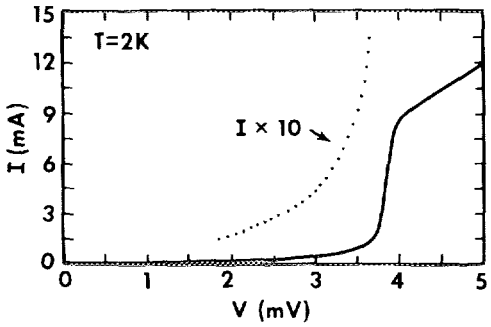

FIG. 3. I-V curve for a NbN_xC_y/native oxide/Pb junction at $T = 2.0$ K. T_c of the base electrode, which is deposited at 200 °C substrate temperature, is 14.1 K. The oxide tunnel barrier is formed by air oxidation for ~20 min. $\Delta(0)$ for Pb is 1.4 meV. The sum-gap voltage is 3.83 mV and the width of the current rise is 0.27 mV. The subgap conductance at 2 mV is 3.8% of the tunneling conductance at 5 mV. The critical current density is ~30 A/cm^2.

V curve in Fig. 3, nevertheless, is typical. Tunneling through NbN_xC_y thermal oxides with $Pb_{0.95}Bi_{0.05}$ or Pb counter electrodes, we find that Δ_{NbN} varies from 2.06 to 2.43 meV as T_c changes from 12.6 to 14.1 K, while $2\Delta/kT_c$ increases from 3.8 to 4.0. Our results for $2\Delta/kT_c$ agree with previous findings[2(a),2(c),4,7] that NbN is a strongly coupled superconductor.

We have also attempted to fabricate all-refractory-metal tunnel junctions. Preliminary results show that a NbN_xC_y native oxide barrier does not withstand the deposition of refractory metal (Nb or NbN_xC_y) counter electrodes, whether or not we use the second ion source (low-energy ions). The junctions show superconducting shorts. The use of alternative barriers is presently under investigation.

In summary, we have fabricated superconducting NbN_xC_y thin films with maximum $T_c \sim 13.2$ K on near-room-temperature Si substrates using a low-energy dual ion-beam sputtering technique. Addition of CH_4 in the sputtering gas is essential for this technique.

The authors thank E. K. Track and G.-J. Cui for collaboration in the studies of Ref. 7 and D. Face for many helpful discussions. We also thank P. Male for TEM pictures, R. Caretta and R. Schulze for the Auger electron spectroscopy (AES) and XPS studies, and J. M. E. Harper, E. J. Cukauskas, and R. B. van Dover for many useful discussions. This research was supported by Office of Naval Research N00014-80-C-0855 and National Science Foundation (NSF) ECS-8305000. AES and XPS studies were conducted at the University of Minnesota NSF Regional Instrumentation Facility under support of NSF CHE-7916206.

[1]rf sputtering methods were utilized by: (a) T. L. Francavilla, S. A. Wolf, and E. F. Skelton, IEEE Trans. Magn. **MAG-17**, 569 (1981); (b) F. Shinoki, A. Shoji, S. Kosaka, S. Takada, and H. Hayakawa, Appl. Phys. Lett. **38**, 285 (1981).

[2]dc magnetron sputtering methods were utilized by: (a) D. D. Bacon, A. T. English, S. Nakahara, F. G. Peters, H. Schreiber, W. R. Sinclair, and R. B. van Dover, J. Appl. Phys. **54**, 6509 (1983); (b) M. Hikita, K. Takei, and M. Igarashi, J. Appl. Phys. **54**, 7066 (1983); (c) J. C. Villegier, L. Vieux-Rochaz, M. Goniche, P. Renard, and M. Vabre, IEEE Trans. Magn. **MAG-21**, 498 (1985); (d) R. T. Kampwirth, D. W. Capone, II, K. E. Gray, and A. Vicens, IEEE Trans. Magn. **MAG-21**, 459 (1985); (e) S. Thakoor, J. L. Lamb, A. P. Thakoor, and S. K. Khanna, J. Appl. Phys. **58**, 4643 (1985).

[3]rf magnetron sputtering methods were utilized by: (a) E. J. Cukauskas, W. L. Carter, S. B. Qadri, and E. F. Skelton, IEEE Trans. Magn. **MAG-21**, 505 (1985); (b) E. J. Cukauskas, W. L. Carter, and S. B. Qadri, J. Appl. Phys. **57**, 2538 (1985).

[4]M. Gurvitch, J. P. Remeika, J. M. Rowell, J. Geerk, and W. P. Lowe, IEEE Trans. Magn. **MAG-21**, 509 (1985).

[5]J. R. Gavaler, J. Talvacchio, and A. I. Braginski, Adv. Cryo. Eng. **32**, 627 (1986).

[6]For previous uses of dual ion-beam sputtering techniques see C. Weissmantel, Thin Solid Films **32**, 11 (1976) and J. M. E. Harper, J. J. Cuomo, and H. T. G. Hentzell, Appl. Phys. Lett. **43**, 547 (1983).

[7]L.-J. Lin, E. K. Track, G.-J. Cui, and D. E. Prober, Physica B **135**, 220 (1985); E. K. Track, L.-J. Lin, G.-J. Cui, and D. E. Prober, Adv. Cryo. Eng. **32**, 635 (1986); G.-J. Cui, L.-J. Lin, E. K. Track, and D. E. Prober, in *Workshop on the Josephson Effect: Trends and Achievement*, edited by A. Barone (World Scientific, Torino, Italy, to be published); T_c values up to 11.9 K have been obtained in subsequent work by E. K. Track with high-energy ions (unpublished).

[8]H. Jones, O. Fischer, and G. Bongi, Solid State Commun. **14**, 1061 (1974); R. W. Ralston, MIT Lincoln Lab., Internal Report ESD-TR-85-317, 1985.

[9]D. W. Face, S. T. Ruggiero, and D. E. Prober, J. Vac. Sci. Technol. A **1**, 326 (1983).

[10]Ion Tech Inc., Fort Collins, Colorado.

[11]Commonwealth Scientific Corporation, Alexandria, Virginia.

[12]R. W. Guard, J. W. Savage, and D. G. Swarthout, Trans. Metall. Soc. AIME **239**, 643 (1967).

[13]Electronic Space Products International, Westlake Village, California.

[14]T. Yamashita, K. Hamasaki, Y. Kodaira, and T. Komata, IEEE Trans. Magn. **MAG-21**, 932 (1985).